Discovery of a potent, selective, and orally available PI3Kδ inhibitor for the treatment of inflammatory diseases

Contents

1. Experimental part Chemistry:

Reagents, starting materials, and solvents were purchased from commercial suppliers and used as received. Concentration or evaporation refers to evaporation under vacuum using a Büchi rotatory evaporator. Reaction products were purified, when necessary, by flash or reverse phase chromatography in a Biotage SP1® or Isolera® automatic purification systems with the solvent system indicated.

Purity and MS identification of all the described compounds was performed in a Waters 2795 system coupled to a 2996 Diode array detector and to a Waters ZQ mass spectrometer detector or in a Waters Acquity UPLC system coupled to a SQD mass spectrometer detector. The injection volume was 5 microliter on the HPLC and 0.5 microliter on the UPLC. Chromatograms were processed at 210 nM or 254 nM. Mass spectra of the chromatograms were acquired using positive and negative electrospray ionization. The mobile phase was formic acid (0.4 mL), ammonia (0.1 mL), methanol (500 mL) and acetonitrile (500 mL) (B) and formic acid (0.5 mL), ammonia (0.125 mL) and water (1000 mL) (A) and a gradient between 0 to 95% of B was used. Columns: HPLC: Waters Symmetry (2.1x50mm, 3.5 μm); UPLC: ACQUITY UPLC BEH C-18 (2.1x50mm, 1.7 μm). All reported compounds showed a purity >95% by UPLC/MS.

^{1}H Nuclear Magnetic Resonance Spectra were recorded on a Varian Mercury plus operating at a frequency of 400MHz. Samples were dissolved in the specified deuterated solvent. Tetramethylsilane was used as reference. ^{13}C-NMR spectra were performed in a Varian VNMR spectrometer at 150 MHz equipped with a cold probe.

High resolution mass spectrum was obtained by positive electrospray ionisation in an Agilent time of flight system.

Experimental details and characterization of all described compounds are reported in an Almirall's patent application (WO2012146666).

Characterization of compounds

2-((6-Amino-9*H*-purin-9-yl)methyl)-5-methyl-3-o-tolylpyrrolo[2,1-*f*][1,2,4]triazin-4(3*H*)-one (2)

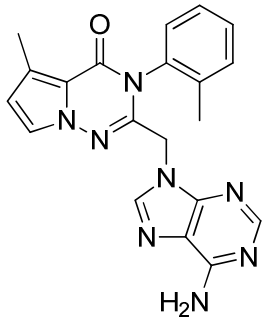

LRMS (m/z): 387 $(M+1)^+$.

2-(1-(6-Amino-9*H*-purin-9-yl)ethyl)-5-methyl-3-phenylpyrrolo[2,1-*f*][1,2,4]triazin-4(3*H*)-one (3)

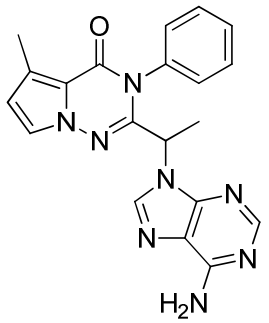

LRMS (m/z): 387 $(M+1)^+$.
^{1}H NMR (400 MHz, DMSO) δ 8.03 (s, 1H), 7.94 (s, 1H), 7.61 (dd, J = 6.7, 1.8 Hz, 1H), 7.55 (d, J = 2.7 Hz, 1H), 7.49 (td, J = 7.6, 1.3 Hz, 1H), 7.30 (tt, J = 7.5, 1.2 Hz, 1H), 7.19 (s, 2H), 7.09 (td, J = 7.7, 1.4 Hz, 1H), 6.76 (d, J = 8.0 Hz, 1H), 6.45 (dd, J = 2.7, 0.7 Hz, 1H), 5.44 (q, J = 6.8 Hz, 1H), 2.39 (s, 3H), 1.68 (d, J = 6.8 Hz, 3H).

***(S)*-2-(1-(9*H*-Purin-6-ylamino)ethyl)-3-phenylpyrrolo[2,1-*f*][1,2,4]triazin-4(3*H*)-one (4)**

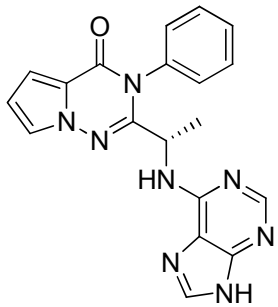

LRMS (m/z): 373 $(M+1)^+$.
^{1}H NMR (400 MHz, DMSO) δ 12.92 (s, 1H), 8.19 – 7.95 (m, 3H), 7.68 – 7.42 (m, 4H), 7.29 (d, J = 17.2 Hz, 1H), 7.17 (s, 1H), 6.93 (dd, J = 4.3, 1.6 Hz, 1H), 6.58 (dd, J = 4.2, 2.7 Hz, 1H), 4.95 – 4.69 (m, 1H), 1.45 (d, J = 6.7 Hz, 3H).

***(S)*-2-(1-(2-Amino-9*H*-purin-6-ylamino)ethyl)-3-phenylpyrrolo[2,1-*f*][1,2,4]triazin-4(3H)-one (5)**

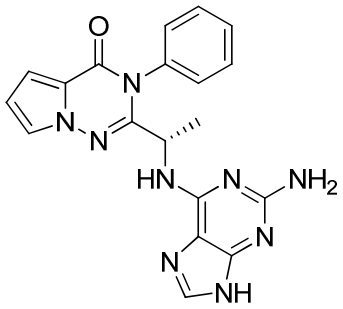

LRMS (m/z): 388 $(M+1)^+$.
^{1}H NMR (400 MHz, DMSO) δ 12.07 (s, 1H), 8.17 (s, 1H), 7.67 (s, 1H), 7.63 – 7.56 (m, 2H), 7.51 (s, 2H), 7.46 – 7.28 (m, 2H), 6.93 (dd, J = 4.3, 1.6 Hz, 1H), 6.57 (dd, J = 4.3, 2.7 Hz, 1H), 5.57 (s, 2H), 4.77 (s, 1H), 1.37 (d, J = 6.8 Hz, 3H).

***(S)*-3-Phenyl-2-(1-(pyrazolo[1,5-a]pyrimidin-7-ylamino)ethyl)pyrrolo[2,1-*f*][1,2,4]triazin-4(3*H*)-one (6)**

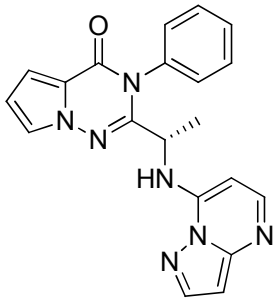

LRMS (m/z): 372 $(M+1)^+$.
^{1}H NMR (400 MHz, DMSO) δ 8.22 (d, J = 7.9 Hz, 1H), 8.09 (d, J = 2.1 Hz, 1H), 7.93 (d, J = 5.2 Hz, 1H), 7.76 – 7.70 (m, 1H), 7.55 (d, J = 7.9 Hz, 1H), 7.45 (t, J = 7.5 Hz, 1H), 7.22 (dd, J = 12.8, 7.2 Hz, 2H), 6.97 (dd, J = 4.2, 1.5 Hz, 1H), 6.87 (t, J = 7.5 Hz, 1H), 6.63 (dd, J = 4.1, 2.8 Hz, 1H), 6.41 (d, J = 2.1 Hz, 1H), 5.59 (d, J = 5.3 Hz, 1H), 4.62 – 4.47 (m, 1H), 1.53 (d, J = 6.5 Hz, 3H).

***(S)*-2-(1-(7*H*-Pyrrolo[2,3-d]pyrimidin-4-ylamino)ethyl)-3-phenylpyrrolo[2,1-*f*][1,2,4]triazin-4(3*H*)-one (7)**

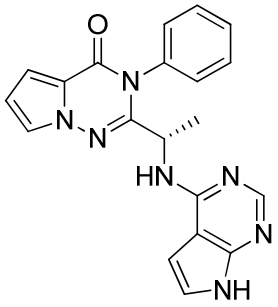

LRMS (m/z): 372 $(M+1)^+$.
^{1}H NMR (400 MHz, DMSO) δ 11.53 (s, 1H), 7.99 (s, 1H), 7.88 (br s, 1H), 7.62 (m, 1H), 7.57 – 7.46 (m, 3H), 7.34 (t, J = 7.2 Hz, 1H), 7.20 (t, J = 7.4 Hz, 1H), 7.10 (s, 1H), 6.95 (dd, J = 4.2, 1.6 Hz, 1H), 6.59 (dd, J = 4.9, 2.1 Hz, 2H), 4.93 – 4.69 (m, 1H), 1.45 (d, J = 6.7 Hz, 3H).

_(S)_-2-(1-(5-Fluoro-7_H_-pyrrolo[2,3-d]pyrimidin-4-ylamino)ethyl)-3-phenylpyrrolo[2,1-_f_][1,2,4]triazin-4(3_H_)-one (8)

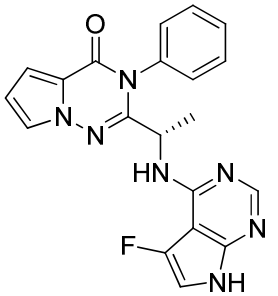

LRMS (m/z): 390 $(M+1)^+$.
^{1}H NMR (400 MHz, DMSO) δ 11.39 (s, 1H), 7.94 (s, 1H), 7.68 – 7.64 (m, 1H), 7.52 (d, J = 8.4 Hz, 1H), 7.43 (m, 2H), 7.25 (m, 2H), 7.14 (td, J = 7.8, 0.8 Hz, 1H), 7.06 (t, J = 2.4 Hz, 1H), 6.94 (dd, J = 4.3, 1.6 Hz, 1H), 6.60 (dd, J = 4.2, 2.7 Hz, 1H), 4.97 (p, J = 6.7 Hz, 1H), 1.45 (d, J = 6.7 Hz, 3H

_(S)_-2-(1-(6-Amino-5-fluoropyrimidin-4-ylamino)ethyl)-3-phenylpyrrolo[2,1-_f_][1,2,4]triazin-4(3_H_)-one (9)

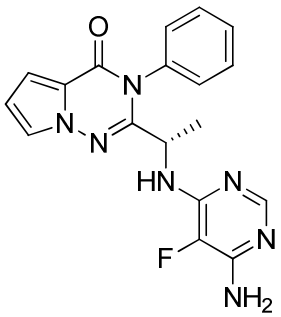

LRMS (m/z): 366 $(M+1)^+$.

^{1}H NMR (400 MHz, DMSO) δ 7.70 – 7.29 (m, 7H), 7.18 (d, 1H), 6.94 (dd, 1H), 6.59 (dd, 1H), 6.36 (br s, 2H), 4.71 – 4.55 (m, 1H), 1.36 (d, 3H).

***(S)*-2-(1-(6-Amino-5-(trifluoromethyl)pyrimidin-4-ylamino)ethyl)-3-phenylpyrrolo[2,1-*f*][1,2,4]triazin-4(3*H*)-one (10)**

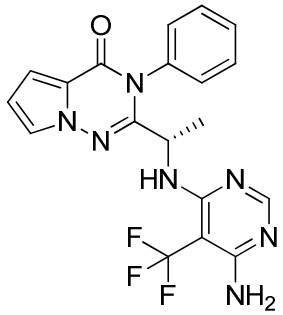

LRMS (m/z): 416 $(M+1)^+$.
^{1}H NMR (400 MHz, DMSO) δ 7.79 (s, 1H), 7.68 – 7.62 (m, 1H), 7.53 – 7.44 (m, 2H), 7.41 – 7.30 (m, 3H), 6.94 (dd, J = 4.2, 1.6 Hz, 1H), 6.74 (br s, 2H), 6.65 (dd, J = 6.8, 1.7 Hz, 1H), 6.60 (dd, J = 4.2, 2.7 Hz, 1H), 5.02 – 4.85 (m, 1H), 1.35 (d, J = 6.6 Hz, 3H).

***(S)*-4-Amino-6-(1-(4-oxo-3-phenyl-3,4-dihydropyrrolo[2,1-*f*][1,2,4]triazin-2-yl)ethylamino)pyrimidine-5-carbonitrile (11)**

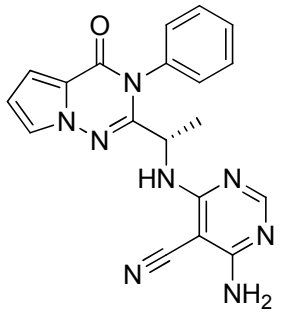

LRMS (m/z): 373 $(M+1)^+$.
^{1}H NMR (400 MHz, DMSO) δ 7.76 (s, 1H), 7.73 – 7.64 (m, 2H), 7.52 – 7.46 (m, 1H), 7.43 (ddd, J = 8.0, 4.6, 2.3 Hz, 1H), 7.38 – 7.26 (m, 3H), 7.20 (s, 2H), 6.95 (dd, J = 4.3, 1.7 Hz, 1H), 6.61 (dd, J = 4.3, 2.7 Hz, 1H), 4.99 – 4.77 (m, 1H), 1.37 (d, J = 6.7 Hz, 3H).

***(S)*-2-(1-(4,6-diamino-1,3,5-triazin-2-ylamino)ethyl)-3-phenylpyrrolo[2,1-*f*][1,2,4]triazin-4(3*H*)-one (12)**

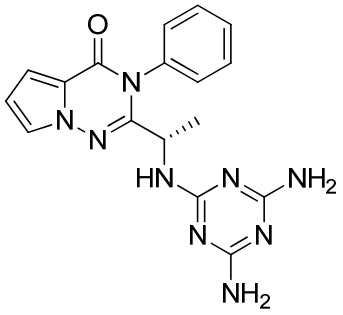

LRMS (m/z): 364 $(M+1)^+$.
^{1}H NMR (400 MHz, DMSO) δ 7.65 – 7.57 (m, 2H), 7.45 (m, 4H), 6.91 (dd, J = 4.3, 1.7 Hz, 1H), 6.83 (d, J = 7.4 Hz, 1H), 6.56 (dd, J = 4.3, 2.7 Hz, 1H), 5.99 (br s, 4H), 4.48 (p, J = 6.6 Hz, 1H), 1.20 (d, J = 6.8 Hz, 3H).

_(S)_-2-(1-(6-Aminopyrimidin-4-ylamino)ethyl)-3-phenylpyrrolo[2,1-_f_][1,2,4]triazin-4(3_H_)-one (13)

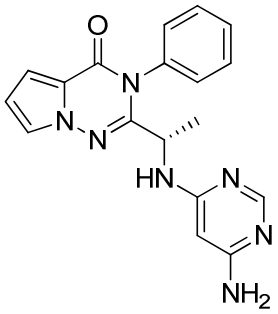

LRMS (m/z): 348 $(M+1)^+$.
^{1}H NMR (400 MHz, DMSO) δ 7.80 (s, 1H), 7.64 – 7.57 (m, 1H), 7.55 – 7.47 (m, 3H), 7.47 – 7.38 (m, 2H), 7.19 (s, 1H), 6.93 (dd, J = 4.2, 1.5 Hz, 1H), 6.58 (dd, J = 4.3, 2.7 Hz, 1H), 6.12 (s, 2H), 5.39 (s, 1H), 4.48 (s, 1H), 1.30 (d, J = 6.8 Hz, 3H).

_(S)_-2-(1-(9_H_-Purin-6-ylamino)propyl)-3-phenylpyrrolo[2,1-_f_][1,2,4]triazin-4(3_H_)-one (14)

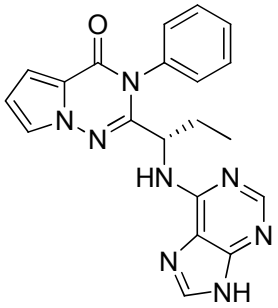

LRMS (m/z): 387 $(M+1)^+$.

^{1}H NMR (400 MHz, DMSO) δ 12.92 (s, 1H), 8.10 (m, 2H), 7.94 (s, 1H), 7.60 (s, 1H), 7.53-7.34 (m, 4H), 6.93 (dd, 1H), 6.64 - 6.54 (m, 1H), 4.65 (s, 1H), 1.98 (m, 2H), 0.77 (t, 3H).

***(R)*-2-(1-(9*H*-Purin-6-ylamino)propyl)-3-phenylpyrrolo[2,1-*f*][1,2,4]triazin-4(3*H*)-one (15)**

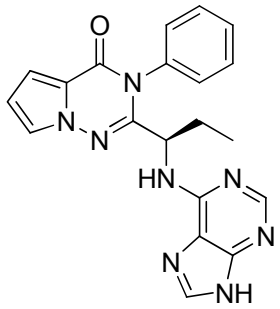

LRMS (m/z): 387 $(M+1)^+$.
^{1}H NMR (400 MHz, DMSO) δ 12.88 (s, 1H), 8.11 (m, 2H), 7.97 (s, 1H), 7.62 - 7.56 (m, 1H), 7.56 - 7.41 (m, 3H), 7.40 (s, 1H), 7.29 (s, 1H), 6.92 (dd, J = 4.2, 1.4 Hz, 1H), 6.56 (dd, J = 4.2, 2.7 Hz, 1H), 4.65 (s, 1H), 1.95 (m, 2H), 0.75 (t, J = 7.0 Hz, 3H).

***(S)*-4-Amino-6-(1-(4-oxo-3-phenyl-3,4-dihydropyrrolo[2,1-*f*][1,2,4]triazin-2-yl)propylamino)pyrimidine-5-carbonitrile (16)**

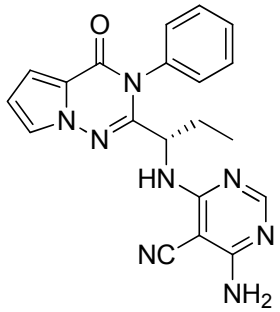

LRMS (m/z): 387 $(M+1)^+$.
^{1}H NMR (400 MHz, DMSO) δ 7.79 (s, 1H), 7.67 (s, 1H), 7.60 (d, J = 7.2 Hz, 1H), 7.48 (d, J = 3.5 Hz, 2H), 7.40 – 7.29 (m, 3H), 7.23 (s, 2H), 6.95 (d, J = 2.8 Hz, 1H), 6.64 – 6.57 (m, 1H), 4.68 (dd, J = 13.3, 7.3 Hz, 1H), 1.86 (ddt, J = 28.8, 13.9, 7.1 Hz, 2H), 0.75 (t, J = 7.2 Hz, 3H).

***(S)*-4-Amino-6-(3-hydroxy-1-(4-oxo-3-phenyl-3,4-dihydropyrrolo[2,1-*f*][1,2,4]triazin-2-yl)propylamino)pyrimidine-5-carbonitrile (17)**

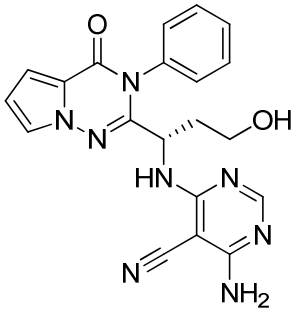

LRMS (m/z): 403 $(M+1)^+$.
^{1}H NMR (400 MHz, DMSO) δ 7.84 (s, 1H), 7.74 – 7.57 (m, 2H), 7.53 – 7.32 (m, 5H), 7.24 (br s, 2H), 6.94 (dd, 1H), 6.60 (dd, 1H), 4.92 – 4.79 (m, 1H), 4.53 (t, 1H), 3.46 – 3.34 (m, 2H), 2.12 – 1.99 (m, 1H), 1.98 – 1.87 (m, 1H).

***(S)*-4-Amino-6-(2-hydroxy-1-(4-oxo-3-phenyl-3,4-dihydropyrrolo[2,1-*f*][1,2,4]triazin-2-yl)ethylamino)pyrimidine-5-carbonitrile (18)**

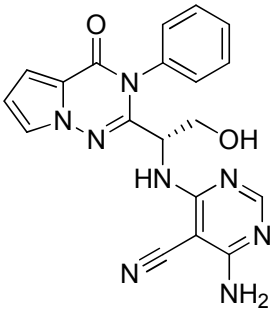

LRMS (m/z): 389 $(M+1)^+$.
^{1}H NMR (400 MHz, DMSO) δ 7.82 (s, 1H), 7.67 (dd, 1H), 7.50 – 7.24 (m, 8H), 6.93 (dd, 1H), 6.59 (dd, 1H), 4.95 (t, 1H), 4.80 – 4.74 (m, 1H), 3.79 (dt, 1H), 3.55 (dt, 1H).

4-Amino-6-(3,3,3-trifluoro-1-(4-oxo-3-phenyl-3,4-dihydropyrrolo[2,1-*f*][1,2,4]triazin-2-yl)propylamino)pyrimidine-5-carbonitrile (19)

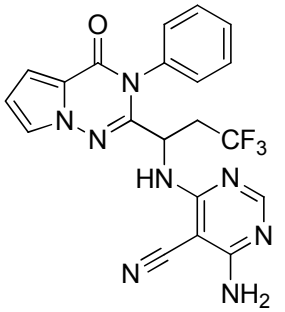

LRMS (m/z): 441 $(M+1)^+$.

^{1}H RMN (400 MHz, DMSO) δ 7.94 (d, 1H), 7.84 (s, 1H), 7.69 (dd, 1H), 7.57 – 7.46 (m, 2H), 7.38 (ddd, 4H), 6.97 (dd, 1H), 6.63 (dd, 1H), 5.22 (dd, 1H), 3.09 – 2.91 (m, 2H).

_(S)_-4-Amino-6-(2-(4-oxo-3-phenyl-3,4-dihydropyrrolo[2,1-_f_][1,2,4]triazin-2-yl)pyrrolidin-1-yl)pyrimidine-5-carbonitrile (20)

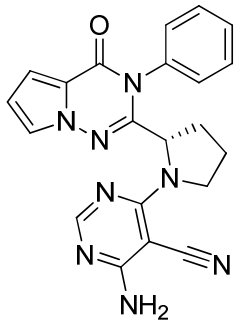

LRMS (m/z): 399 $(M+1)^+$.
^{1}H NMR (400 MHz, DMSO) δ 8.03 (s, 1H), 7.69 - 7.46 (m, 6H), 7.28 (s, 2H), 6.91 (dd, 1H), 6.53 (m, 1H), 2.26 - 2.08 (m, 3H), 2.00 - 1.90 (m, 2H), 1.86 - 1.74 (m, 2H).

_(S)_-4-Amino-6-(4,4-difluoro-2-(4-oxo-3-phenyl-3,4-dihydropyrrolo[2,1-_f_][1,2,4]triazin-2-yl)pyrrolidin-1-yl)pyrimidine-5-carbonitrile (21)

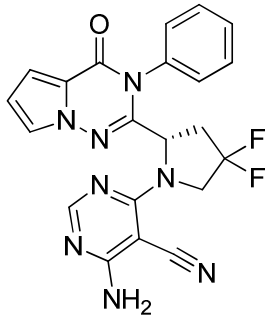

LRMS (m/z): 435 $(M+1)^+$.
^{1}H NMR (400 MHz, DMSO) δ 8.14 (s, 1H), 7.80 – 7.40 (m, 7H), 6.95 (dd, 1H), 6.57 (dd, 1H), 4.91 (s, 1H), 4.53 – 4.21 (m, 2H), 3.01 – 2.74 (m, 1H), 2.48 – 2.40 (m, 1H).

4-Amino-6-(1-(4-oxo-3-phenyl-3,4-dihydropyrrolo[2,1-_f_][1,2,4]triazin-2-yl)cyclopropylamino)pyrimidine-5-carbonitrile (22)

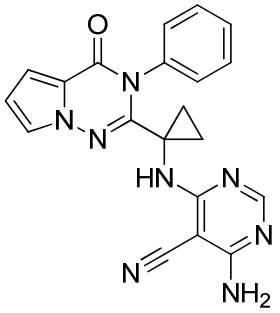

LRMS (m/z): 385 $(M+1)^+$.
^{1}H NMR (400 MHz, DMSO) δ 7.99 (s, 1H), 7.68 (s, 1H), 7.59 – 7.45 (m, 3H), 7.39 – 7.15 (m, 4H), 6.90 (dd, 1H), 6.58 (dd, 1H), 5.38 (dd, 1H), 1.83 – 1.69 (m, 2H), 1.15 – 1.03 (m, 2H).

_(S)_-4-Amino-6-(1-(5-methyl-4-oxo-3-phenyl-3,4-dihydropyrrolo[2,1-_f_][1,2,4]triazin-2-yl)ethylamino)pyrimidine-5-carbonitrile (23)

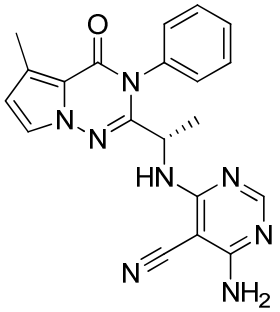

LRMS (m/z): 387 $(M+1)^+$.
^{1}H NMR (400 MHz, DMSO) δ 13.02 (s, 1H), 8.39 (d, 1H), 8.17 (s, 1H), 8.14 (s, 1H), 7.60 (dd, 2H), 7.54 (t, 2H), 7.42 (t, 1H), 7.32 (t, 1H), 6.96 (dd, 1H), 6.59 (dd, 1H), 5.22 (s, 1H), 3.17 – 2.97 (m, 2H).

_(S)_-4-Amino-6-(1-(5-(hydroxymethyl)-4-oxo-3-phenyl-3,4-dihydropyrrolo[2,1-_f_][1,2,4]triazin-2-yl)ethylamino)pyrimidine-5-carbonitrile (24)

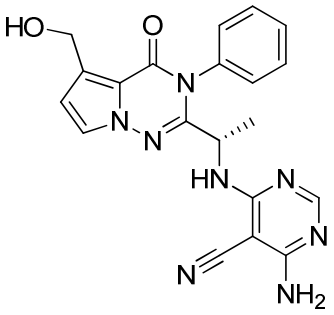

LRMS (m/z): 403 $(M+1)^+$.

^{1}H NMR (400 MHz, DMSO) δ 8.08 (s, 1H), 7.64 – 7.53 (m, 3H), 7.51 – 7.45 (m, 1H), 7.38 – 7.30 (m, 2H), 6.48 (d, 1H), 5.76 (d, 1H), 5.50 (br s, 2H), 5.11 – 4.98 (m, 1H), 4.81 (s, 2H), 1.42 (d, 3H).

_(S)_-4-Amino-6-(1-(5-fluoro-4-oxo-3-phenyl-3,4-dihydropyrrolo[2,1-*f*][1,2,4]triazin-2-yl)ethylamino)pyrimidine-5-carbonitrile (25)

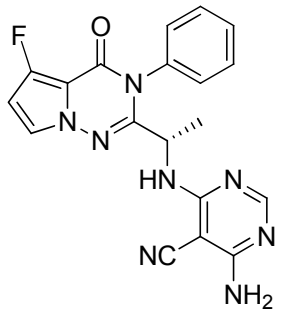

LRMS (m/z): 391 $(M+1)^+$.
^{1}H NMR (400 MHz, CDCl3) δ 10.73 (s, 1H), 8.33 (s, 1H), 7.98 (br s, 1H), 7.57 - 7.41 (m, 5H), 7.38 – 7.31 (m, 1H), 7.14 (dd, 1H), 6.52 (m, 1H), 5.18 (s, 1H), 1.50 (d, 3H).

_(S)_-4-Amino-6-(1-(4-oxo-3-phenyl-5-(trifluoromethyl)-3,4-dihydropyrrolo[2,1-*f*][1,2,4]triazin-2-yl)ethylamino)pyrimidine-5-carbonitrile (27)

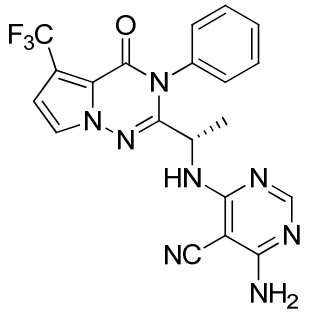

LRMS (m/z): 441 $(M+1)^+$.
^{1}H NMR (400 MHz, DMSO) δ 7.83 (d, J = 2.8 Hz, 1H), 7.75 (s, 1H), 7.62 (d, J = 6.8 Hz, 1H), 7.53 (d, J = 7.9 Hz, 1H), 7.44 (m, 1H), 7.37 - 7.17 (m, 5H), 6.99 (d, J = 2.8 Hz, 1H), 4.89 (p, J = 6.5 Hz, 1H), 1.36 (d, J = 6.6 Hz, 3H).

_(S)_-4-Amino-6-(1-(6-fluoro-4-oxo-3-phenyl-3,4-dihydropyrrolo[2,1-*f*][1,2,4]triazin-2-yl)ethylamino)pyrimidine-5-carbonitrile (28)

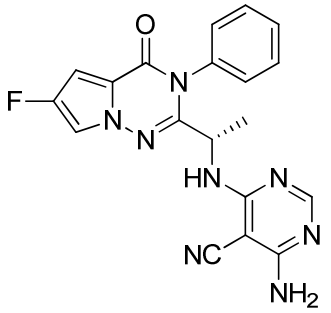

LRMS (m/z): 391 $(M+1)^+$.
^{1}H NMR (400 MHz, DMSO) δ 7.85 (d, 1H), 7.76 (s, 1H), 7.68 (d, 1H), 7.55 – 7.09 (m, 7H), 6.85 (d, 1H), 4.95 – 4.83 (m, 1H), 1.36 (d, 3H).

_(S)_-4-Amino-6-(1-(7-methyl-4-oxo-3-phenyl-3,4-dihydropyrrolo[2,1-_f_][1,2,4]triazin-2-yl)ethylamino)pyrimidine-5-carbonitrile (29)

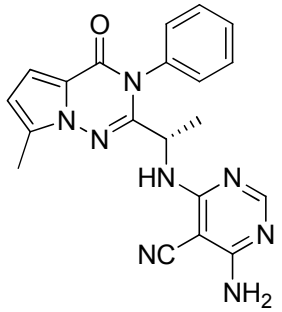

LRMS (m/z): 387 $(M+1)^+$.
^{1}H NMR (400 MHz, DMSO) δ 7.75 (s, 1H), 7.63 (d, J = 7.1 Hz, 1H), 7.49 - 7.38 (m, 2H), 7.27 (m, 5H), 6.88 (d, J = 4.1 Hz, 1H), 6.44 (d, J = 3.9 Hz, 1H), 5.02 - 4.90 (m, 1H), 2.47 (s, 3H).

_(S)_-2-(1-(6-Amino-5-cyanopyrimidin-4-ylamino)ethyl)-4-oxo-3-phenyl-3,4-dihydropyrrolo[2,1-_f_][1,2,4]triazine-7-carbonitrile (30)

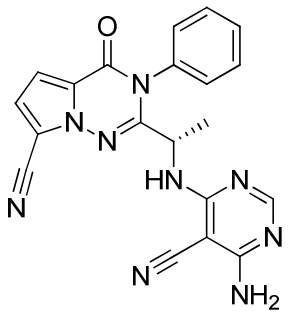

LRMS (m/z): 398 $(M+1)^+$.

***(S)*-4-Amino-6-(1-(4-oxo-3-phenyl-7-(trifluoromethyl)-3,4-dihydropyrrolo[2,1-*f*][1,2,4]triazin-2-yl)ethylamino)pyrimidine-5-carbonitrile (31)**

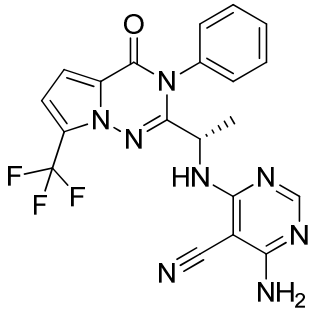

LRMS (m/z): 441 $(M+1)^+$.

***(S)*-4-amino-6-(1-(4-oxo-3-phenyl-3,4-dihydroimidazo[2,1-*f*][1,2,4]triazin-2-yl)ethylamino)pyrimidine-5-carbonitrile (32)**

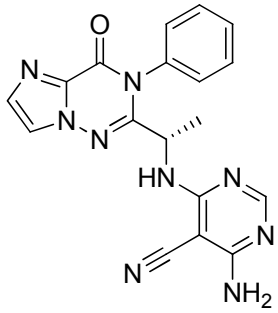

LRMS (m/z): 374 $(M+1)^+$.
^{1}H RMN (400 MHz, DMSO) δ 8.14 (s, 1H), 7.78 (s, 1H), 7.64 (d, 1H), 7.60 (s, 1H), 7.55 (d, 1H), 7.47 (dd, 1H), 7.40 - 7.28 (m, 2H), 7.25 (s, 2H), 4.90 (m, 1H), 1.39 (d, 3H).

Synthesis of Compound 26

3-Bromo-N-phenyl-1-(phenylsulfonyl)-1*H*-pyrrole-2-carboxamide
In a three-necked round-bottom flask aniline (1.57 mL, 17.20 mmol) was dissolved in 80 mL of toluene under inert atmosphere. To this solution was added trimethy aluminium (7.82 mL, 15.64 mmol) and the mixture was stirred at room temperature during 10 minutes. Afterwards, a solution methyl 3-bromo-1-(phenylsulfonyl)-1*H*-pyrrole-2-carboxylate (2.0 g, 5.81 mmol) in 20 mL of toluene were added and the reaction mixtures was heated at 80ºC for 3h. Next, the mixture was allowed to cool to room temperature and 20-30 mL of water was added to hydrolyze unreacted trimethyl aluminium and a 0,5M aqueous solution of disodium tartrate dihydrate was also added. After stirring for a while, the two layers were separated and the aqueous phase was extracted with ethyl acetate. The organic mixture was washed with the same 0,5M aqueous solution of disodium tartrate dehydrate (200 mL), water and brine, dried

and concentrated in vacuum to afford 2.7 g of a residue that was used in the following step without further purification.

LRMS (m/z): 405, 407 $(M+1)^+$.

3-Bromo-N-phenyl-1*H*-pyrrole-2-carboxamide

To a solution of 3-bromo-N-phenyl-1-(phenylsulfonyl)-1*H*-pyrrole-2-carboxamide (2.70 g of crude material) in 50 mL of methanol was added 15 mL of an aqueous 1N solution of sodium hydroxide and the mixture was stirred at room temperature during 1.5 h. At the end of this period, no starting material was detected and the reaction was elaborated in the following way: methanol was evaporated and a precipitate was formed which was filtered off and washed several times with water. The solid was dried in the vacuum oven to afford 1.14g and used in the following step without further purification.

LRMS (m/z): 265, 267 $(M+1)^+$.

1-Amino-3-bromo-N-phenyl-*1H*-pyrrole-2-carboxamide

In a 100 mL three-necked flask it was placed 11 mL of a 28% aqueous solution of sodium hydroxide, 4.1 mL of a 28% ammonium hydroxide solution, 1.23 g of ammonium chloride and 0.12 mL of Aliquat 336. Afterwards, a solution of 3-bromo-N-phenyl-1*H*-pyrrole-2-carboxamide (1.11 g, 4.19 mmol) in 30 mL of diethyl ether and 30 mL of methyl *tert*-butyl ether was added and placed at 0ºC affording a suspension. Over this suspension, a 10% aqueous solution of sodium hypochlorite (26 mL) was added drop wise with vigorous stirring maintaining the temperature during 20 min. more. Subsequently, the reaction mixture was stirred at room temperature during a further 1.5 h producing the consumption of the starting material. Next, the reaction crude was diluted with ethyl acetate until no suspended material was observed. The layers were separated and the organic phase was washed with a 25% aqueous solution of sodium thiosulphate, water and brine, dried (Na_2SO_4) and concentrated under vacuum to give a residue that was triturated with hexane to produce a solid (780 mg, 67% yield) after filtration.

LRMS (m/z): 280, 282 $(M+1)^+$.

***(S)-tert*-Butyl 1-(3-bromo-2-(phenylcarbamoyl)-1*H*-pyrrol-1-ylamino)-1-oxopropan-2-ylcarbamate**

810 mg (2.89 mmol) of 1-amino-3-bromo-N-phenyl-1*H*-pyrrole-2-carboxamide and 656 mg (3.47 mmol) of *(S)*-2-(*tert*-butoxycarbonylamino)propanoic acid (purchased from Aldrich) and 1.2 eq of EDC·HCl were dissolved in a mixture of 30 mL of THF and 10 mL of dichloromethane. The resulting solution was heated at 55 ºC overnight. Then the solvents were evaporated and the crude residue was taken up in dichloromethane and washed with an aqueous solution of sodium bicarbonate and brine. The organic layer was dried over magnesium sulphate, filtered and the solvent was evaporated. The crude product was purified by flash chromatography in hexane/ethyl acetate to afford 670 mg (49% yield) of the title compound.

LRMS (m/z): 306, 308 $(M+1)^+$.

***(S)-tert*-Butyl 1-(5-bromo-4-oxo-3-phenyl-3,4-dihydropyrrolo[2,1-*f*][1,2,4]triazin-2-yl)ethylcarbamate**

A solution of bromine (2.3 eq) in dichloromethane (2.5 mL) was added dropwise to a solution of triphenylphosphine (2.3 eq) in dichloromethane (7 mL) under nitrogen. The solution was stirred for 30 min, and triethylamine (3.7eq) and a solution of *((S)-tert*-butyl 1-(3-bromo-2-(phenylcarbamoyl)-1*H*-pyrrol-1-ylamino)-1-oxopropan-2-ylcarbamate (670 mg, 1.48 mmol) in 4 ml of dichloromethane were added. The reaction mixture was stirred at room temperature for 3.5 h, and then, volatiles were removed under reduced pressure and the residue was triturated with toluene affording a solid that was removed by filtration. The filtrate was concentrated to dryness under reduced pressure and the residue was redissolved in 20 mL of a 7M methanolic solution of ammonia and stirred overnight at 80 ºC in a sealed vessel. The solvent was then evaporated and the residue was purified by flash chromatography in hexane/ethyl acetate to afford 500 mg (78% yield) of the title compound.

LRMS (m/z): 433, 435 $(M+1)^+$.

***(S)-tert*-butyl 1-(5-cyano-4-oxo-3-phenyl-3,4-dihydropyrrolo[2,1-*f*][1,2,4]triazin-2-yl)ethylcarbamate**

A mixture of methyl *(S)-tert*-butyl 1-(5-bromo-4-oxo-3-phenyl-3,4-dihydropyrrolo[2,1-f][1,2,4]triazin-2-yl)ethylcarbamate (238 mg, 0.55 mmol), dicyanozinc (129mg, 1.10mmol) and Tetrakis(triphenylphosphine)palladium(0) (64mg, 0.06mmol) in DMF, was heated at 120ºC in a sealed tub overnight with stirring. Next day, ethyl acetate was added and filtered thought Celite®. Phases were separated and the aqueous layer extracted with more ethyl acetate. The combined organic layer was dried (Na_2SO_4) and concentrated in vacuum to give 580 mg of a residue that was purified by flash chromatography (hexane/ethyl acetate) to obtain 119 mg (57% yield) of the title compound.

LRMS (m/z): 380 $(M+1)^+$.

***(S)*-2-(1-Aminoethyl)-4-oxo-3-phenyl-3,4-dihydropyrrolo[2,1-*f*][1,2,4]triazine-5-carbonitrile**

((S)-tert-butyl1-(5-cyano-4-oxo-3-phenyl-3,4-dihydropyrrolo[2,1-f][1,2,4]triazin-2-yl)ethylcarbamate (119 mg, 0.31 mmol) was dissolved in 2ml of dioxane and 2 ml of a 4M hydrogen chloride solution were added. The mixture was stirred at room temperature overnight. Reaction mixture was then concentrated and the residue dissolved in ethyl acetate and a 2N solution of NaOH. The organic layer was separated and the aqueous layer extracted with more ethyl acetate. The combined organic layer was dried over magnesium sulphate and concentrated to dryness. 67mg (77% yield) of the desired compound were obtained.

LRMS (m/z): 280 $(M+1)^+$.

***(S)*-2-(1-(6-Amino-5-cyanopyrimidin-4-ylamino)ethyl)-4-oxo-3-phenyl-3,4-dihydropyrrolo[2,1-*f*][1,2,4]triazine-5-carbonitrile (Compound 26)**

0.14 mmol of *(S)*-2-(1-aminoethyl)-4-oxo-3-phenyl-3,4-dihydropyrrolo[2,1-f][1,2,4]triazine-5-carbonitrile and 0.15 mmol of 4-amino-6-chloropyrimidine-5-carbonitrile (prepared according to the procedure described in WO2010151735A2) and 0.41mmol of diisopropylethylamine were heated in *tert*-butanol (2 mL) for 21 hours. Then the solvent was removed under vacuum and the crude product was purified by flash chromatography (0-10% methanol in dichloromethane) to give the title compound (74% yield) as a white solid.

LRMS (m/z): 398 $(M+1)^+$.

^{1}H NMR (400 MHz, DMSO) δ 7.89 (d, J = 3.0 Hz, 1H), 7.78 (s, 1H), 7.62 (d, J = 6.7 Hz, 1H), 7.54 - 7.44 (m, 2H), 7.39 - 7.30 (m, 3H), 7.24 (br s, 1H), 7.21 (d, J = 3.0 Hz, 1H), 4.91 (p, J = 6.7 Hz, 1H), 1.38 (d, J = 6.7 Hz, 3H).

^{13}C NMR (150 MHz, DMSO) δ 164.5 (1C), 161.4 (1C), 159.5 (1C), 153.4 (1C), 152.8 (1C), 134.6 (1C), 129.4-129.7 (2C), 128.9-130.0 (2C), 128.8 (1C), 122.6 (1C), 115.9 (1C), 114.9-115.6 (2C), 90.4 (1C), 68.3 (1C), 47.2 (1C), 18.2 (1C).

HRMS (ESI^+) calcd for $C_{20}H_{16}N_9O$ $[M+H]^+$ 398.1472, $C_{20}H_{19}N_{10}O$ $[M+NH_4]^+$ 415.1738, $C_{20}H_{15}N_9NaO$ $[M+Na]^+$ 420.1292, found 398.147, 415.1733, 420.1281. All the errors were lower than 0.7ppm.

2. *In vitro* characterization:

2.1. PI3K Alpha, Beta, Delta and Gamma enzymatic inhibiton assays

A biochemical HTRF assay was used to determine the compound potency on the different PI3K isoforms. PI-3 Kinase HTRF kit (ref. #33-037) and the different PI3K recombinant isoforms (PI3K p110α/p85α, PI3K p110β/p85α, PI3K p110δ/p85α and PI3K p110γ) expressed in insect cells (ref. #14-602, ref. #14-603, ref.#14-604, ref.#15-558 for Alpha, Beta, Delta and Gamma respectively) were purchased from Millipore. Briefly, the compounds were pre-incubated with the enzyme for 30 min prior to triggering the catalytic reaction. Concentration of PIP2 (included in the kit) and ATP (sigma Aldrich, ref. #A7699) were used at their respective Km. Time of assay and enzyme concentration were optimized to work in the linear range. Stop and detection mixtures were used as specified in the Millipore PI-3 Kinase kit.

Dose-response curves were plotted by using a four parameter log equation according to model 204 in Excel fit software.

2.2. Determination of PI3K delta-dependent cellular potency on THP-1 cells

THP-1 cells in serum free medium were seeded in a 96w plate . Compounds were preincubated for 30min at 37ºC and then Akt phosphorylation was induced by the addition of MCSF for 3min at room temperature. The reaction was stopped with cold PBS, cells were centrifuged and the cell pellet was lysed with the solution provided in the ELISA kit (Cell Signaling, #7135). Following centrifugation, supernatants were collected and Akt (Thr308) phosphorylation was analysed by ELISA according to the manufacturer's instructions. Luminescence signals were recorded in a Luminoskan equipment.

2.3. Determination of PI3K Beta-dependent cellular potency

HUVEC cells were purchased from Lonza (ref. CC-2519A) and cultured as specified by the provider. Cells were incubated with compounds during 15 minutes followed by stimulation with S1P (Sigma ref. #S966) at its EC_{80} during 5 minutes at 37ºC in order to induce activation of PI3Kβ. Levels of pAKT were determined following the HTRF Phospho AKT kit specifications (Cisbio, ref. 64AKSPEH) for detection of Phospho-Serine 473. HTRF reading was performed after 4h of incubation on the Envision plate reader.

2.4. Determination of Inhibitory activity on human B cells from PBMC or human whole blood

Compound activity on B cell activation induced by anti-IgD was investigated in isolated human PBMCs or whole blood. In both cases, the percentage of CD19+ cells expressing CD69 was determined as a direct measure of PI3Kδ engagement.

PBMCs were extracted from heparinized human peripheral blood by a ficoll gradient. The isolated cells were resuspended in RPMI supplemented with 2% autologous plasma and dispensed in a 96w plate.

Cells were incubated with vehicle (DMSO) or compound for 30min at 37ºC prior to activation by the addition of anti-IgD for 2h at 37ºC. Cells were stained with FITC-labeled (BD Biosciences) anti-CD19 and PE-labeled anti-CD69 (BD Biosciences) for 15min at room temperature in the dark. Following two washes with PBS with 1% FBS and 0.1% sodium azide, samples were analysed by flow cytometry in a FACSCalibur flow cytometer.

For determination of activity on human whole blood, 40 μL of heparinized human peripheral blood was dispensed in a 96w plate and incubated with vehicle (DMSO) or compound for 30min at 37ºC prior to activation by the addition of anti-IgD for 2h at 37ºC and stained with labeled antibodies as above. Erythrocytes were lysed and staining was fixed by the addition of FACS Lysis reagent (BD Biosciences). After an incubation of 15min, samples were centrifuged and supernatants discarded. Lysis reagent was added again for 10min.

Following two washes with PBS with 1% FBS and 0.1% sodium azide, samples were analysed by flow cytometry in FACSCalibur. Quadrants were adjusted to the vehicle-treated non-stimulated cells so that no more than 5% cells were positive in basal conditions.

Percentage of inhibition versus vehicle stimulated wells was calculated and plotted using a four parameter log equation.

2.5. General selectivity

Activity of compound **26** was assessed at a single concentration of 10 μM in

- 81 GPCR receptors, 8 ion channels and 5 transporters (Cerep)
- 273 protein and lipid kinases (Millipore, Invitrogen and ProQinase)

No significant inhibition was found at the concentration tested.

3. In vivo characterization

Animal care was in compliance with the European Committee Directive 2010/63/EU and the Spanish and autonomous Catalan laws (Real Decreto 53/2013 and Decret 214/1997). Experimental procedures were reviewed by the Animal-Welfare Body of Almirall and approved by the competent authority.

3.1. ConA induced IL-2 increase in rats

The objective of this study was to assess the activity of LAS191954 on the inhibition of Concanavalin A (ConA) induced increases in plasma interleukin-2 (IL-2) in Wistar rats. A dose-response curve was assessed to obtain an ID_{50} of the compound.

Male Wistar Rats (170-220g) were weighed and randomly assigned to 6 dose groups, corresponding to Control-Vehicle, ConA-Vehicle and treatment groups. Animals were then orally administered by gavage (10 ml/kg) with either vehicle (0.5% w/v of MC + 0.1% v/v Tween 80 in distilled water for Control-Vehicle and ConA-Vehicle groups) or compounds (LAS191954 0.03, 0.1, 0.3, 1 and 3 mg/kg or LAS191257 at 0.3, 1, 3, 10 and 30mg/kg).

One hour later, animals (excluding Control-Vehicle group) were challenged with an intravenous bolus of of ConA (10 mg/kg) in PBS, in the lateral tail vein (1 ml/kg).

Ninety minutes after the ConA challenge, animals were anesthetized with isofluorane, blood samples obtained from heart and the animals were then humanely euthanized.

All blood samples were collected in Eppendorf tubes at 4°C, and centrifuged at 4000 r.p.m. for 8 minutes (5415R Eppendorf, Hamburg, Germany). Plasma samples were stored at -20°C for subsequent analysis.

A commercial IL-2 ELISA (Quantikine® Rat IL-2 ELISA R2000, R&D Systems, Abingdon, UK) was used to determine IL-2 concentration in plasma of every animal.

Results are expressed as mean of the percentage of reduction of circulating IL-2 versus the difference between Control-Vehicle and ConA-Vehicle groups.

% of IL-2 inhibition=

$$100 - \frac{(\text{IL-2 in test compound} - \text{Mean IL-2 in Control-Vehicle group}) * 100}{\text{Mean IL-2 in ConA-Vehicle group} - \text{Mean IL-2 in Control-Vehicle group}}$$

The ID_{50} value was calculated using a Graph Pad Prism 5.00 (Graph Pad Software Inc., San Diego, CA, USA) by fitting a sigmoidal curve fit to the data.

3.2. Ovalbumin (OVA) induced eosinophilia in BN rats

Brown Norway (BN) male rats weighing 225-275g were intraperitoneally sensitized on days 0, 14 and 21 with OVA 100µg and Imject Alum 20mg in 1 ml of saline. On day 28, animals were treated with 10ml/kg of vehicle (0.5% methylcellulose + 0.1% tween 80 in water), LAS 191954 (0.1, 0.3, 1, 3 mg/kg) or Idelalisib (5, 15, 50 mg/kg) orally. LAS 191954 and Idelalisib were administered 1h before and 6h after an aerosol challenge of OVA (1%, 60min) or saline.

Bronchoalveolar lavage (BAL) samples were obtained 24h after the challenge. Animals were terminally anaesthetized with a dose of pentobarbital (85 mg kg-1, 0.15 ml) by i.p. route. The trachea was cannulated and the lungs lavaged twice with 3 ml of PBS containing 5% fetal bovine serum. BAL eosinophils were counted by the haematology analyser Sysmex XT-2000iV (Sysmex Corporation, Kobe, Japan) and by microscopy (after cytospin preparation of BAL samples, the differential count was performed considering cell morphological and staining properties).

Data were expressed as ID50 of percentage of eosinophilia inhibition (medians) and plotted using GraphPad Prism 6.04 (GraphPad Software, San Diego, CA, USA).

4. ADME characterization

4.1. PAMPA

The PAMPA assay measures permeability across an artificial membrane. This method provides an *in vitro* model for passive diffusion. Passive diffusion is an important factor in determining transport through the gastrointestinal tract, penetration of the blood brain barrier, as well as transport across cell membranes. Permeability can also be influenced by several other mechanisms including paracellular transport and active uptake or efflux which are not assessed in PAMPA. Therefore, PAMPA provides a simplistic approach to permeability by only measuring a single mechanism. This avoids the complexities of active transport/efflux and enables the compounds to be ranked on a single permeability property.

The test compound (20 μM) is added to the donor compartment of a 96 well plate. The permeation of compound across an artificial hexadecane membrane is quantified by LC-MS/MS after a five hour incubation at room temperature..

The apparent permeability for each compound (P_{app}) is calculated from the following equation:

$$P_{app} = C \times -\ln\left(1 - \frac{[\,drug_{acceptor}\,]}{[\,drug_{equilibrium}\,]}\right)$$

$$\text{where} \qquad C = \frac{V_D \times V_A}{(V_D + V_A) \times area \times time}$$

Where V_D and V_A are the volumes of the donor and acceptor compartments, respectively, area is surface area of the membrane multiplied by the porosity and the equilibrium drug concentration is the concentration of test compound in the total volume of the donor and acceptor compartments.

4.2. Microsomal metabolism

The liver is the main organ of drug metabolism in the body. Subcellular fractions such as liver microsomes are useful *in vitro* models of hepatic clearance as they contain many of the drug metabolising enzymes found in the liver. Microsomes are easy to prepare and can be stored for long periods of time. They are easily adaptable to high throughput screens which enable large numbers of compounds to be screened rapidly and inexpensively.
The metabolic stability is conducted in microsomes at a single time-point (30 min). Microsomes (1 mg/ml) are incubated with the test compound (5μM) at 37°C in the presence of the co-factor, NADPH, which initiates the reaction. After the 30 min incubation period, the reaction is terminated by the addition of Acetonitrile. Following centrifugation, the amount of parent compound in the supernatant is quantified by UPLC-MS/MS. The percentage of metabolism is calculated by comparing the peak area of the parent compound at 30 min versus zero time point control.

4.3. Plasma Protein Binding (PPB)

Equilibrium dialysis is used to determine the extent of binding of a compound to plasma proteins. A semi-permeable membrane separates a protein-containing compartment from a protein-free compartment. The system is allowed to equilibrate at 37°C. The test compound present in each compartment is quantified by LC-MS/MS.
The extent of binding is reported as PPB (%) and fraction unbound (fu) values which are calculated as detailed below;

$$Drug_{unbound}(\%) = \frac{Conc(bufferchamber)}{Conc(samplechamber)} \times 100$$

$$PPB(\%) = 100 - Drug_{unbound}(\%)$$

$$fu = 1 - \left(\frac{PC - PF}{PC}\right)$$

PC = Test compound concentration in protein-containing compartment.
PF = Test compound concentration in protein-free compartment.

4.4. Plasma stability

To determine the stability of new chemical entities in plasma, the test compound is incubated with plasma (final incubation concentration 5 µM), at 37 ºC at five different time points (0, 15 min, 30 min, 1h, 2h, 4h and 24h). The reaction is terminated by the addition of Acetonitrile. Following centrifugation, the concentration of test compound in the supernatant is quantified by UPLC-MS/MS. The percentage of test compound remaining at the individual time points relative to the 0 minute sample is then reported.
The Ln (concentration) is plotted against time, and the gradient of the line determined. The half-life of the test compound is calculated as follows:

Elimination rate constant (K)= (-gradient)
t1/2=Ln2/K

4.5. CYP inhibition

The main cytochrome P450 isoforms (CYP1A, CYP2C9, CYP2C19, CYP2D6 and CYP3A4) are investigated in the Cytochrome P450 Inhibition assay. Isoform-specific substrates (CYP1A: Ethoxyresorufin *O*-deethylation; , CYP2C9: Diclofenac 4-hydroxylation, CYP2C19: S-mephenytoin 4-hydroxylation, CYP2D6: Dextromethorphan *O*-demethylation and CYP3A4: Testosterone 6ß-hydroxylation) are incubated individually with human liver microsomes and a range of test compound concentrations (typically 1- 25 µM). At the end of the incubation, the formation of metabolite is monitored by UPLC-MS/MS at each of the test compound concentrations.
A decrease in the formation of the metabolites compared to vehicle control is used to calculate an IC_{50} value (test compound concentration which produces 50% inhibition).
A known specific positive control inhibitors for each of the isoform assays is run.

4.6. GSH trapping

This assay is used to detect glutathione conjugates of a test compound due to formation of a reactive metabolite. The incubation is performed with human liver microsomes in the presence of NADPH and GSH. Microsomes (1 mg/ml) are incubated with the test compound (25 µM) at 37°C in the presence of NADPH and GSH. After the 60 min incubation period, the reaction is terminated by the addition of Acetonitrile. Following centrifugation the samples are analysed by UPLC-MS, comparing the 60 min versus the 0 min time-point control samples. The presence of GSH-conjugates is determined by mass spectrometry analysis, following the neutral loss of 129 characteristic of the glutathione cleavage.

4.7. Pharmacokinetics in rats

Pharmacokinetic studies were performed in male Wistar rats. Catheters were surgically implanted into the carotid artery of the animals and connected to a Culex system. The test substance was administered intravenously through the tail vein or orally by oral gavage. Serial blood samples were collected at various timepoints from the carotid artery into tubes containing sodium heparin as anti-coagulant. Samples were centrifuged to separate plasma and kept frozen until final processing.

4.8. Pharmacokinetics in dogs

Pharmacokinetic studies were performed in male Beagle dogs. The test substance was administered intravenously as a bolus into the cephalic vein or orally by oral gavage. Serial blood samples were collected at various timepoints from the jugular vein into tubes containing sodium heparin as anti-coagulant. Samples were centrifuged to separate plasma and kept frozen until final processing.

5. Experimental methods for X-ray structure of human PI3Kδ in complex with compound 11

Protein Production

Suitable constructs for human PI3Kδ expression had been previously established by PROTEROS. Expression of human PI3Kδ was performed according to previously established protocols. A purification protocol was established and homogeneous protein was produced in preparative amounts. The protein was purified comprising affinity and gel filtration chromatography steps. This procedure yielded homogenous protein with a purity greater 95 % as judged from coomassie stained SDS-PAGE.

Crystallisation

The purified protein was used in crystallisation trials employing both, a standard screen with approximately 1200 different conditions, as well as crystallisation conditions identified using literature data. Conditions initially obtained have been optimised using standard strategies, systematically varying parameters critically influencing crystallisation, such as temperature, protein concentration, drop ratio, and others. These conditions were also refined by systematically varying pH or precipitant concentrations.

Data Collection and Processing

The application of the Free Mounting System (FMS) was necessary to obtain well diffracting crystals. The crystals were transferred to the N2 cryo-stream at 100K. The Free Mounting System (FMS) is a proprietary device to improve the analysis and handling of protein crystals. At room temperature, the protein crystal is mounted "freely" with a cryo loop into an adjustable and reproducible flow of humidified air or gas (Kiefersauer et al., J. Appl. Cryst., 33, 1223-1230, 2000). The "free" mounting not only allows further manipulation of the crystal during the X-ray based analysis but also is a valuable tool for freezing of protein crystals. The X-ray diffraction

data have been collected from complex crystals of human PI3Kδ with the ligand at the SWISS LIGHT SOURCE (SLS, Villigen, Switzerland) using cryogenic conditions. The crystals belong to space group P 21 21 21. Data were processed using the programmes XDS and SCALA

Table 5. Data collection and processing statistics for Compound **11**

Ligand	Compound 11
X-ray source	PXI/X06SA (SLS[1])
Wavelength [Å]	0.9999
Detector	PILATUS 6M
Temperature [K]	100
Space group	P 21 21 21
Cell: a; b; c; [Å]	92.49; 113.21; 144.32
α; β; γ; [◦]	90.0; 90.0; 90.0
Resolution [Å]	2.85 (3.18-3.00)[2]
Unique reflections	36274 (4956)[2]
Multiplicity	6.5 (6.8)[2]
Completeness [%]	99.8 (100.0)[2]
Rsym [%] [3]	4.0 (39.3)[2]
Rmeas [%] [4]	4.7 (46.4)[2]
I/σ(I)	7.7 (2.0)[2]
Mean(I)/sd [5]	21.1 (4.0)[2]

[1] SWISS LIGHT SOURCE (SLS, Villigen, Switzerland)

[2] values in parenthesis refer to the resolution bin with R_{sym} = 39.3 %.

[3] $$R_{sym} = \frac{\sum_h \sum_i^{n_h} |\widehat{I}_h - I_{h,i}|}{\sum_h \sum_i^{n_h} I_{h,i}} \text{ with } \widehat{I}_h = \frac{1}{n_h} \sum_i^{n_h} I_{h,i}$$

where $I_{h,i}$ is the intensity value of the ith measurement of h

[4] $$R_{meas} = \frac{\sum_h \sqrt{\frac{n_h}{n_h - 1}} \sum_i^{n_h} |\widehat{I}_h - I_{h,i}|}{\sum_h \sum_i^{n_h} I_{h,i}} \text{ with } \widehat{I}_h = \frac{1}{n_h} \sum_i^{n_h} I_{h,i}$$

where $I_{h,i}$ is the intensity value of the ith measurement of h

[5] calculated from independent reflections

Structure Modelling and Refinement

The phase information necessary to determine and analyse the structure was obtained by molecular replacement. A previously solved structure of human PI3Kδ was used as a search model. Subsequent model building and refinement was performed according to standard protocols with the software packages CCP4 and COOT. For the calculation of the free R-factor, a measure to cross-validate the correctness of the final model, about 2.8 % of measured

reflections were excluded from the refinement procedure (see Table 6). TLS refinement (using REFMAC5, CCP4) has been carried out, which resulted in lower R-factors and higher quality of the electron density map. The ligand parameterisation and generation of the corresponding library files were carried out with CORINA. The water model was built with the "Find waters"-algorithm of COOT by putting water molecules in peaks of the F_o-F_c map contoured at 3.0 σ followed by refinement with REFMAC5 and checking all waters with the validation tool of COOT. The criteria for the list of suspicious waters were: B-factor greater 80 Å^2, 2F_o-F_c map less than 1.2 σ, distance to closest contact less than 2.3 Å or more than 3.5 Å. The suspicious water molecules and those in the active site (distance to inhibitor less than 10 Å) were checked manually. The occupancy of side chains, which were in negative peaks in the F_o-F_c map (contoured at -3.0 σ), were set to zero and subsequently to 0.5 if a positive peak occurred after the next refinement cycle. The Ramachandran Plot of the final model shows 90.8 % of all residues in the most favoured region, 8.7 % in the additionally allowed region, and 0.5 % in the generously allowed region. No residues are found in the disallowed region (Table 6).
Statistics of the final structure and the refinement process are listed in Table 6.

Table 6. Refinement statistics for Compound **11**[1]

Ligand	Compound 11
Resolution [Å]	89.08-2.85
Number of reflections (working/test)	35097 / 997
Rcryst [%]	25.6
Rfree[%] [2]	30.9
Total number of atoms:	
Protein	8811
Water	
Ligand	28
Deviation from ideal geometry: [3]	
Bond lengths [Å]	0.009
Bond angles [°]	1.05
Bonded B's [Å2] [4]	2.6
Ramachandran plot: [5]	
Most favoured regions [%]	90.8
Additional allowed regions [%]	8.7
Generously allowed regions [%]	0.5
Disallowed regions [%]	0.0

[1] Values as defined in REFMAC5, without sigma cut-off
[2] Test-set contains 2.8 % of measured reflections
[3] Root mean square deviations from geometric target values
[4] Calculated with MOLEMAN
[5] Calculated with PROCHECK

Figure 4. Overall structure of human PI3Kδ containing the ligand (compound **11**) shown as ribbon diagram

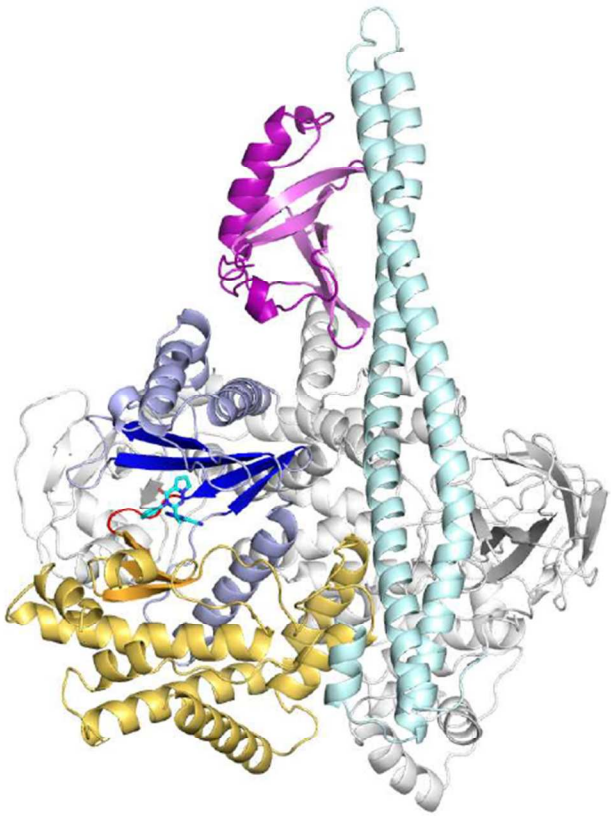

Figure 5. Binding pocket of human PI3Kδ containing the ligand (compound **11**) shown in the two orientations rotated by 90 degrees.

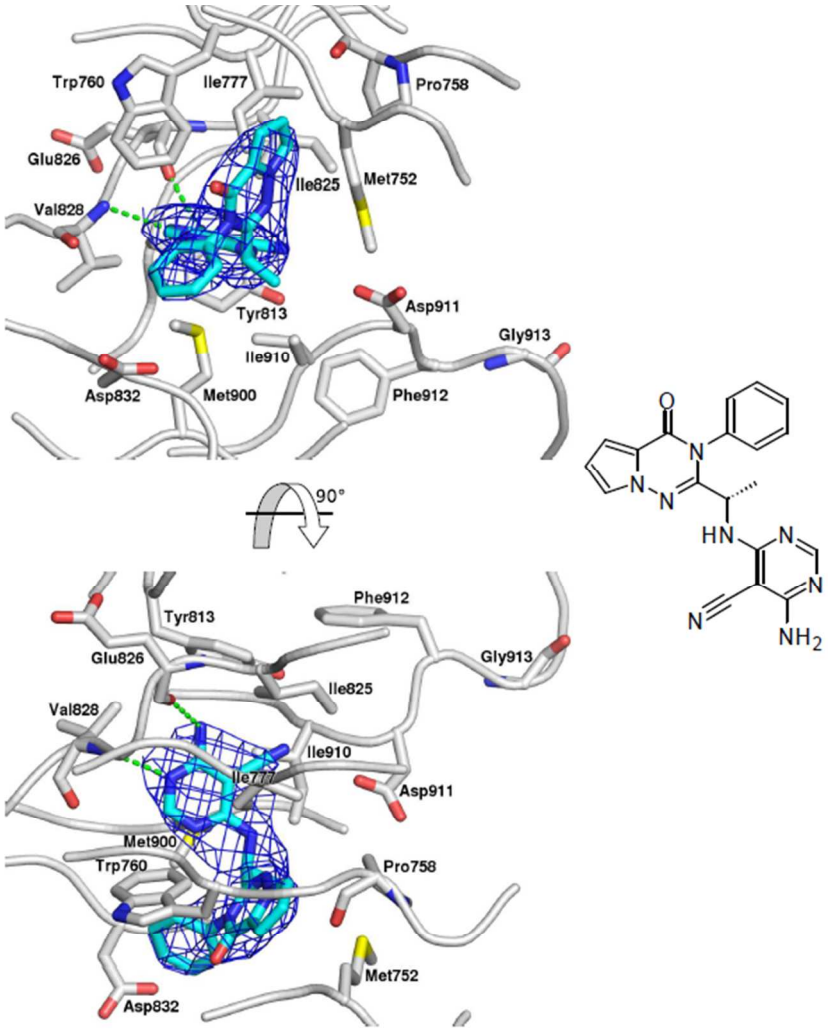
Trp760
Ile777
Pro758
Glu826
Ile825
Met752
Val828
Tyr813
Asp911
Gly913
Ile910
Asp832
Met900
Phe912
90°
Tyr813
Phe912
Glu826
Gly913
Ile825
Val828
Ile910
Ile777
Asp911
Met900
Trp760
Pro758
Met752
Asp832
O
N
N
N
HN
N
N
N
NH2